Spectroscopic studies in open quantum systems

I. Rotter,[1] E. Persson,[2] K. Pichugin,[3] and P. Šeba[3,4]
[1]*Max-Planck-Institut für Physik komplexer Systeme, D-01187 Dresden, Germany*
[2]*Institut für Theoretische Physik, Technische Universtität Wien, A-1040 Wien, Austria*
[3]*Institute of Physics, Czech Academy of Sciences, Cukrovarnicka 10, Prague, Czech Republic*
[4]*Department of Physics, Pedagogical University, Hradec Kralove, Czech Republic*
(Received 14 February 2000)

The Hamiltonian $\mathcal{H}$ of an open quantum system is non-Hermitian. Its complex eigenvalues $\mathcal{E}_R$ are the poles of the S matrix and provide both the energies and widths of the states. We illustrate the interplay between Re($\mathcal{H}$) and Im($\mathcal{H}$) by means of the different interference phenomena between two neighboring resonance states. Level repulsion may occur along the real or imaginary axis (the latter is called resonance trapping). In any case, the eigenvalues of the two states avoid crossing in the complex plane. We then calculate the poles of the S matrix and the corresponding wave functions for a rectangular microwave resonator with a scatter as a function of the area of the resonator as well as of the degree of opening to a waveguide. The calculations are performed by using the method of exterior complex scaling. Re($\mathcal{H}$) and Im($\mathcal{H}$) cause changes in the structure of the wave functions which are permanent, as a rule. The resonance picture obtained from the microwave resonator shows all the characteristic features known from the study of many-body systems in spite of the absence of two-body forces. The effects arising from the interplay between resonance trapping and level repulsion along the real axis are not involved in the statistical theory (random matrix theory).

PACS number(s): 05.45.−a, 05.60.Gg, 03.65.Nk, 85.30.Vw

I. INTRODUCTION

For more than ten years, interference phenomena in open quantum systems have been studied theoretically in the framework of different models. Common to all these studies is the appearance of different time scales as soon as the resonance states start to overlap (see Refs. [1–8], and references in these papers to older works). Some of the states align with the decay channels, and become short lived while the remaining ones decouple to a great deal from the continuum of decay channels and become long lived. The wave functions show permanent changes: they are mixed strongly in the basic wave functions of the corresponding closed system.

In many-body systems the interaction is caused, above all, by two-body forces between the constituents of the system. The additional interaction connected with avoided level crossings is believed, usually, to lead only to an exchange of the wave functions but not to permanent changes of their structure. This conclusion results from many spectroscopic studies on closed systems with discrete states. Recent investigations in the framework of a schematical model [1] showed, however that, in the case of collective resonance states, permanent changes in the wave functions occur due to the interplay between the real and imaginary parts of the different coupling matrix elements.

The mixing of the resonance states of a microwave resonator is not caused by two-body forces. A mixing of the states may occur only as a result of avoided level crossings. It is therefore an interesting question whether or not some permanent mixing in the wave functions of a microwave cavity can arise. In Ref. [9], changes in the structure of wave functions at avoided crossings in a strongly driven (closed) square potential well system were studied. The avoided crossings are shown to lead, in some cases, to temporary changes, and, in other cases, to permanent changes as a function of driving field strength.

The avoided level crossings are related to exceptional points in the complex plane [6]. The coupling induced by avoided level crossings is therefore surely connected with the coupling matrix elements of the discrete states of the closed system to the continuum. In the continuum shell model, these coupling matrix elements are complex [10]. Interferences appear when more than one channel is open. It is therefore possible that interferences of different types may eventually provide a permanent mixing of the wave functions of the resonance states. A similar study of microwave cavities does not exist.

It is the aim of the present paper to study the resonance picture of an open microwave resonator in detail. We show that its characteristic features are the same as those which are known from open many-body quantum systems. This means that not only two-body forces play a role for interaction among the resonance states but also the interaction W via the continuum is important. Neither Re(W) nor Im(W) can be neglected, generally. They are important near avoided crossings in the complex plane and their interplay can not be neglected when Re(W) and Im(W) are of the same order of magnitude. As a result, permanent changes in the structure of the wave functions appear, as a rule. Basic assumptions of the statistical theory (random matrix theory) are fulfilled only when the interferences caused by the Hermitian and anti-Hermitian parts of the Hamiltonian can be neglected to a good approximation. This is the case, e.g., for a Gaussian orthogonal ensemble coupled weakly to the continuum.

In Sec. II of the present paper, the Hamiltonian of an open quantum system and the relation of its eigenvalues to the poles of the S matrix is considered. The formalism can be applied to a many-body system as well as to a microwave resonator. The Hamiltonian is non-Hermitian, and the eigen-

values provide the energies as well as the widths of the states. In Sec. III the avoided crossing of two resonance states is traced. The differences between the mixing of the states due to the Hermitian and anti-Hermitian parts of $\mathcal{H}$ are the central point of discussion. The Hermitian part causes an equilibration of the states in relation to the time scale, which is accompanied by level repulsion along the real axis (energy). In contrast to this, the anti-Hermitian part leads to an attraction of the levels in energy and to a bifurcation of the widths (formation of different time scales). These processes are characteristic of the interplay among resonances which takes place locally in more complicated systems [11].

In Sec. IV, the resonance structure of a rectangular microwave resonator coupled to one lead is studied. Inside the resonator is a circular scatter. Level repulsion in the complex plane appears. This can be seen sometimes as a level repulsion along the real energy axis. In other cases, a bifurcation of the widths occurs. The changes in the structure of the wave functions are permanent, as a rule. Collective states are formed at strong couplings to the lead. The structure of their wave functions has almost nothing in common with the structure of the wave functions of states at small coupling. Together with the collective states, long-lived trapped states appear. The conductance of the microwave resonator is studied after coupling it to a second lead. The conductance peaks are determined by the poles of the S matrix, which move as a function of the coupling strength between cavity and leads. The results are discussed in Sec. V, and some conclusions are drawn in Sec. VI.

II. HAMILTON OPERATOR OF AN OPEN QUANTUM SYSTEM

The function space of an open quantum system consists of two parts: the subspace of discrete states (Q subspace) and the subspace of scattering states (P subspace). The discrete states are states of the closed system which are embedded into the continuum of scattering states. Due to the coupling of the discrete states to the continuum, they can decay, and have a finite lifetime.

Let us define two sets of wave functions by first solving the Schrödinger equation $(H^{\rm cl}-E_R^{\rm cl})\Phi_R^{\rm cl}=0$ for the discrete states of the closed system, and second the Schrödinger equation $(H^{cc}-E^{(+)})\xi_E^c=0$ for the scattering states of the environment. Note that the closed system can be a many-particle quantum system or a system like a microwave resonator. The only condition is that it can be described quantum mechanically by the Hermitian Hamilton operator $H^{\rm cl}$. In the case of the flat microwave resonator, this is possible by using the analogy to the Helmholtz equation. Then the Q and P operators can be defined by

$$Q=\sum_{R=1}^{N}|\Phi_R^{\rm cl}\rangle\langle\Phi_R^{\rm cl}|,\quad P=\sum_{c=1}^{\Lambda}\int_{\epsilon_c}^{\infty}dE|\xi_E^c\rangle\langle\xi_E^c| \tag{1}$$

and $Q\cdot\xi_E^c=0$ and $P\cdot\Phi_R^{\rm cl}=0$. In order to perform spectroscopic studies, we do not use any statistical assumptions (for details, see Ref. [12]).

Assuming $Q+P=1$, we can determine a third wave function by solving the scattering problem $(H^{cc}-E^{(+)})\omega_R=-\Sigma_c\gamma_{Rc}\xi_E^c$ with a source term. The source term is determined by the coupling matrix elements γ_{Rc} between the two subspaces. Further, we identify $H^{\rm cl}$ with $\mathcal{H}_0\equiv QHQ$, where $(H-E)\Psi=0$ is the Schrödinger equation in the total function space $P+Q$. Then the solution $\Psi=P\Psi+Q\Psi$ in the total function space is [12]

$$\Psi=\xi_E^c+\frac{1}{2\pi}\sum_{R=1}^{N}\sum_{R'=1}^{N}(\Phi_R^{\rm cl}+\omega_R)\langle\Phi_R^{\rm cl}|\frac{1}{E-\mathcal{H}}|\Phi_{R'}^{\rm cl}\rangle\gamma_{R'c}$$
$$=\xi_E^c+\sum_{R=1}^{N}\tilde{\Phi}_R\frac{\tilde{\gamma}_{Rc}}{E-\tilde{E}_R+\frac{i}{2}\tilde{\Gamma}_R}. \tag{2}$$

Here

$$\mathcal{H}=\mathcal{H}_0+W \tag{3}$$

is the effective Hamilton operator appearing in the Q subspace due to the coupling to the continuum, $\tilde{\Phi}_R$ are the eigenfunctions of $\mathcal{H}$, and $\tilde{\mathcal{E}}_R\equiv\tilde{E}_R-i/2\tilde{\Gamma}_R$ its eigenvalues. They provide the wave functions, energies, and widths, respectively, of the resonance states. γ_{Rc} are the coupling matrix elements between the discrete states $\Phi_R^{\rm cl}$ and the continuum of scattering states ξ_E^c, while $\tilde{\gamma}_{Rc}$ are those between the resonance states $\tilde{\Phi}_R$ and the continuum. The matrix elements of W consist of the principal value integral and the residuum [12]:

$$W_{R'R}^{\rm ex}=\frac{1}{2\pi}\sum_{c=1}^{\Lambda}\mathcal{P}\int_{\epsilon_c}^{\infty}dE'\frac{\gamma_{Rc}\gamma_{R'c}}{E-E'}-\frac{i}{2}\sum_{c=1}^{\Lambda}\gamma_{Rc}\gamma_{R'c}. \tag{4}$$

Here $c=1,\ldots,\Lambda$ are the channels which open at the energies ϵ_c. They describe the external mixing of two states via the continuum of decay channels. As a rule, both parts $\mathrm{Re}(W)$ and $\mathrm{Im}(W)$ are nonvanishing.

Note that expressions (2), (3), and (4) follow by formal rewriting the Schrödinger equation $(H-E)\Psi=0$, with the only condition that Q and $P=1-Q$ are defined in such a manner that the channel wave functions of the P subspace are uncoupled [12]. Otherwise, the eigenvalues and eigenfunctions of $\mathcal{H}$ have no physical meaning. $\tilde{E}_R,\tilde{\Gamma}_R,\tilde{\gamma}_{Rc}$, and $\tilde{\Phi}_R$ are energy dependent functions, generally.

The resonance part of the S matrix is [12]

$$S_{cc'}^{(\rm res)}=i\sum_{R=1}^{N}\frac{\tilde{\gamma}_{Rc'}\tilde{\gamma}_{Rc}}{E-\tilde{E}_R+\frac{i}{2}\tilde{\Gamma}_R}. \tag{5}$$

We underline that $\tilde{\gamma}_{Rc}$, $\tilde{E}_R$, $\tilde{\Gamma}_R$, and $\tilde{\Phi}_R$ are functions which are calculated inside the formalism. They contain the contributions of $\mathrm{Im}(W)$ and of $\mathrm{Re}(W)$. $\tilde{\gamma}_{Rc}$ and $\tilde{\Phi}_R$ are complex.

III. AVOIDED CROSSING OF TWO RESONANCE STATES

A. Schematical study

In order to illustrate the mutial influence of two neighboring resonance states, we consider the Hamilton operator

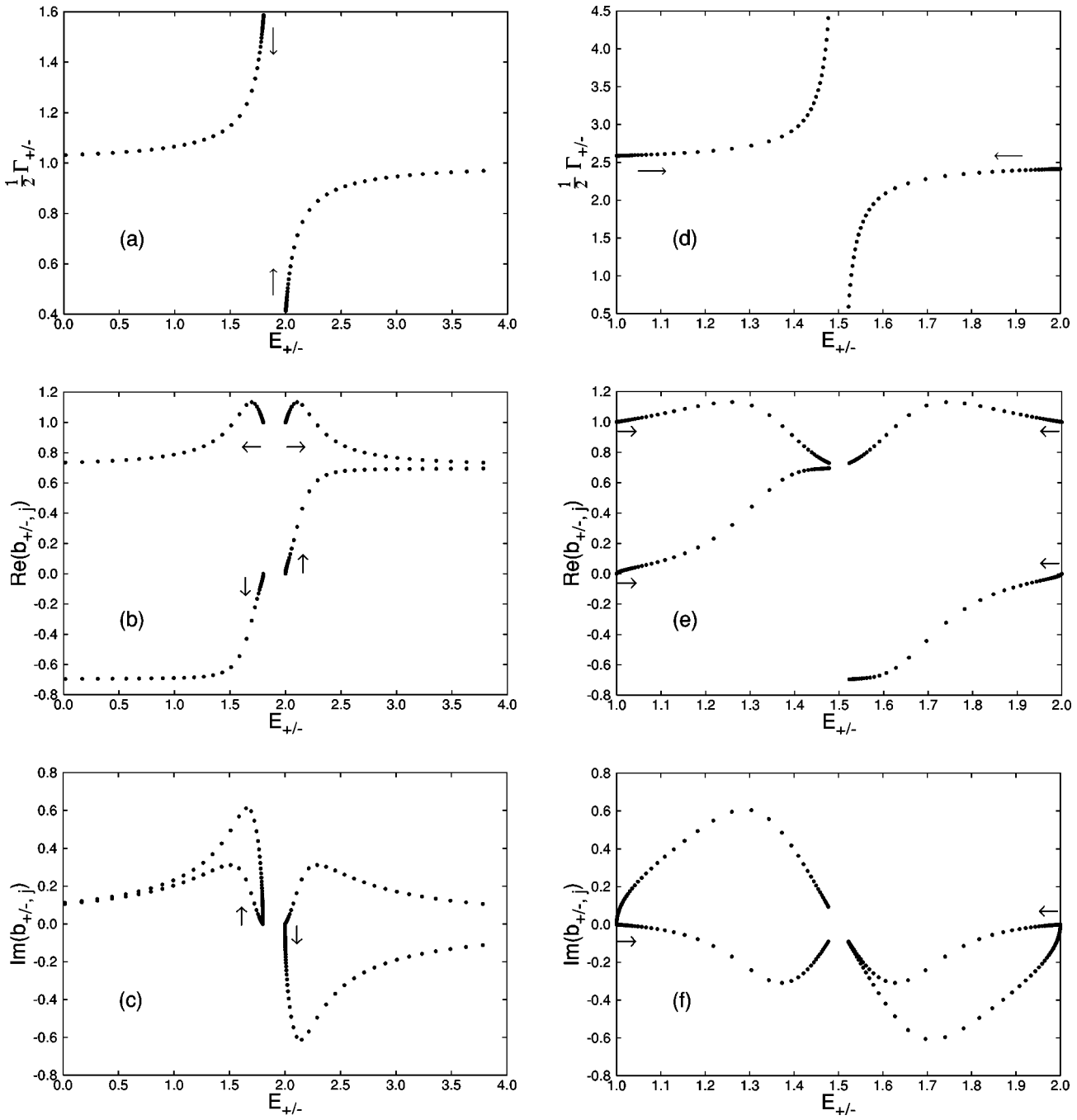

FIG. 1. Eigenvalue picture: motion of the poles of the S matrix in dependence on increasing v_{in} (a) and w_{ex} (d). The mixing of the wave functions $\tilde{\Phi}_{\pm}$ for different v_{in} [(b) and (c)] and w_{ex} [(e) and (f)] which is shown as a function of the energies $E_{\pm}$ of the states. At $v_{\mathrm{in}}=0$ and $w_{\mathrm{ex}}=0$, respectively, $b_{\pm,j}=\delta(\pm,j)$. The arrows indicate the direction of increasing v_{in} and w_{ex}, respectively.

$$\mathcal{H}^{(v)}=\begin{pmatrix}\epsilon_1 & v_{\mathrm{in}}\\ v_{\mathrm{in}} & \epsilon_2\end{pmatrix}\equiv\begin{pmatrix}E_1 & v_{\mathrm{in}}\\ v_{\mathrm{in}} & E_2\end{pmatrix}-\frac{i}{2}\begin{pmatrix}\Gamma_1 & 0\\ 0 & \Gamma_2\end{pmatrix} \qquad (6)$$

which describes two resonance states lying at the energies E_1 and E_2. These two states have widths Γ_1 and Γ_2, respectively, and are coupled by v_{in} (where v_{in} is real). The eigenvalues are

$$\mathcal{E}_{\pm}^{(v)}\equiv E_{\pm}^{(v)}-\frac{i}{2}\Gamma_{\pm}^{(v)}=\frac{\epsilon_1+\epsilon_2}{2}\pm\frac{1}{2}\sqrt{(\epsilon_1-\epsilon_2)^2+4v_{\mathrm{in}}^2}. \qquad (7)$$

When $\Gamma_1\approx\Gamma_2$, the coupling v_{in} of the two states leads to a level repulsion along the real axis.

When Γ_1 and Γ_2 are different from one another, the motion of the eigenvalues as a function of the coupling strength v_{in} is more complicated. Numerical results for such a case are shown in Fig. 1(a). Here the motion of the eigenvalues as a function of increasing v_{in} is indicated by the arrows near $v_{\mathrm{in}}=0$. There is first, up to a certain critical value $v_{\mathrm{in}}^{\mathrm{cr}}$ of the coupling strength, an attraction of the levels along the imaginary axis, which leads to $\Gamma_{+}^{(v)}\approx\Gamma_{-}^{(v)}$. For further increasing coupling strength beyond the critical value $v_{\mathrm{in}}^{\mathrm{cr}}$, the levels repel each other along the real axis in the same manner as in

the case with $\Gamma_1 \approx \Gamma_2$ discussed above. This is the Landau-Zener effect generalized to open quantum systems: the two levels avoid crossing in the complex plane at $v_{\rm in}=v_{\rm in}^{\rm cr}$.

Let us now consider the Hamiltonian with the coupling $iw_{\rm ex}$ ($w_{\rm ex}$ is real) of the two states via the continuum,

$$\mathcal{H}^{(w)}=\begin{pmatrix} \epsilon_1 & iw_{\rm ex} \\ iw_{\rm ex} & \epsilon_2 \end{pmatrix} \equiv \begin{pmatrix} E_1 & 0 \\ 0 & E_2 \end{pmatrix} - \frac{i}{2}\begin{pmatrix} \Gamma_1 & -2w_{\rm ex} \\ -2w_{\rm ex} & \Gamma_2 \end{pmatrix}. \tag{8}$$

In this case, the eigenvalues are

$$\mathcal{E}_{\pm}^{(w)} \equiv E_{\pm}^{(w)} - \frac{i}{2}\Gamma_{\pm}^{(w)} = \frac{\epsilon_1+\epsilon_2}{2} \pm \frac{1}{2}\sqrt{(\epsilon_1-\epsilon_2)^2-4w_{\rm ex}^2}. \tag{9}$$

For $E_1 \approx E_2$, the coupling via the continuum due to $iw_{\rm ex}$ leads to repulsion along the imaginary axis (bifurcation of the widths), i.e., to resonance trapping. Numerical results for $E_1 \not\approx E_2$ are given in Fig. 1(d). They show an avoided crossing of the two levels in an analogous manner as in the case discussed above for $v_{\rm in}$ [Fig. 1(a)]. The attraction of the two levels for $w_{\rm ex} < w_{\rm ex}^{\rm cr}$ takes place, however, along the real axis, and $E_+^{(w)} \approx E_-^{(w)}$ is reached. For $w_{\rm ex} > w_{\rm ex}^{\rm cr}$, the widths of the two states bifurcate.

In both cases, the trajectories for the motion of the eigenvalues in the complex plane as a function of the interaction $v_{\rm in}$ [Fig. 1(a)] and $w_{\rm ex}$ [Fig. 1(d)], respectively, avoid crossing in the complex plane. Figures 1(a) and 1(d) show the avoided crossing of the two resonance states in the complex plane. This occurs at a certain critical value of the coupling strength. Here and in its neighborhood a redistribution between the two states takes place. It is accompanied by the biorthogonality of the eigenfunctions $\tilde{\Phi}_{\pm}$ of $\mathcal{H}$, $B \equiv (1/2)\Sigma_i \langle \tilde{\Phi}_i | \tilde{\Phi}_i \rangle > 1$ where $i=+,-$. The wave functions of the two resonance states become mixed, $\tilde{\Phi}_{\pm}=\Sigma b_{\pm,j}\Phi_j^0$, where Φ_j^0 are the eigenfunctions of $\mathcal{H}^0$, which is the Hamilton operator with vanishing nondiagonal matrix elements ($v_{\rm in}=0$ and $w_{\rm ex}=0$, respectively). In Figs. 1(b) and 1(c) [1(e) and 1(f)], the coefficients $b_{\pm,j}$ are shown as a function of the coupling strength $v_{\rm in}(w_{\rm ex})$ expressed by the corresponding position $E_{\pm}$ of the two states $\tilde{\Phi}_{\pm}$. At vanishing nondiagonal matrix elements, the states are pure, and lie at energies E_1 and E_2, respectively. The arrows indicate the changes of the mixing coefficients $b_{+,j}$ and $b_{-,j}$ with increasing coupling strength. The states remain strongly mixed for coupling strengths beyond the critical one, $|b_{\pm,j}| \to 1/\sqrt{2}$. In the same limit $B \to 1$, i.e., the biorthogonality of the wave functions ($B>1$) is important only in the critical region of the coupling strength.

As it is well known and can be seen from Eq. (7), two interacting discrete states ($v_{\rm in} \neq 0$) cannot cross. In the complex plane, however, the conditions for crossing of two resonance states may be fulfilled. From $\mathcal{E}_+ = \mathcal{E}_-$, it follows that

$$R \equiv (E_1-E_2)^2 - \frac{1}{4}(\Gamma_1-\Gamma_2)^2 + 4(v_{\rm in}^2 - w_{\rm ex}^2) = 0,$$

$$I \equiv (E_1-E_2)(\Gamma_1-\Gamma_2) + 8v_{\rm in}w_{\rm ex} = 0 \tag{10}$$

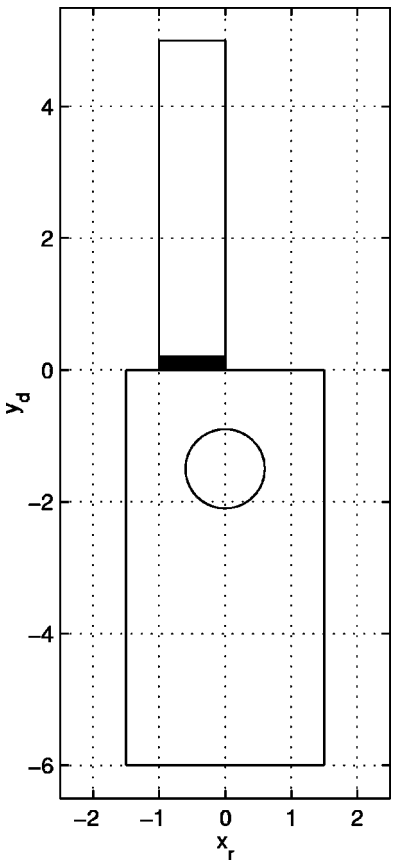

FIG. 2. The resonator. The slide, shown in black, will be opened from the center to both sides ($0.5 \geqslant w \geqslant 0$, where $w=0.5$ (0) corresponds to closed (fully open)). x_r and y_d are given in arbitrary units $[x]$.

for the general case of a complex interaction $v_{\rm in}+iw_{\rm ex}$. These conditions define the critical values of the coupling strength ($v_{\rm in}^{\rm cr}$ and $w_{\rm ex}^{\rm cr}$, respectively) at which the S matrix has a branch point [13].

It is also possible that two resonance states cross along the real or imaginary axis while the crossing is avoided along the other axis. The conditions for such a case with $I=0$ are $R<0$ for crossing along the real axis and $R>0$ for crossing along the imaginary axis. The crossing in the complex plane is avoided, in any case.

From a mathematical point of view, the properties of the system at an avoided crossing in the complex plane (i.e., in regions of the critical coupling strength $v_{\rm in}^{\rm cr}$ and $w_{\rm ex}^{\rm cr}$, respectively) are almost the same: repulsion of the eigenvalues along one axis and attraction along the other axis. The physical meaning is, however, very different: $v_{\rm in}$ causes equilibrium (in relation to the lifetime) and level repulsion along the real axis, while $iw_{\rm ex}$ creates different time scales (bifurcation of the widths) and level attraction along the real axis.

When the coupling contains both $v_{\rm in}$ and $iw_{\rm ex}$, then it depends on the ratio between the two parts whether level repulsion or attraction along the real axis dominates. As a rule, the crossing of states is avoided in the complex plane, and results in a complicated interference picture. The wave functions of the resonance states are mixed permanently in the set of the eigenfunctions of the Hamiltonian $\mathcal{H}_0$ of the corresponding closed system.

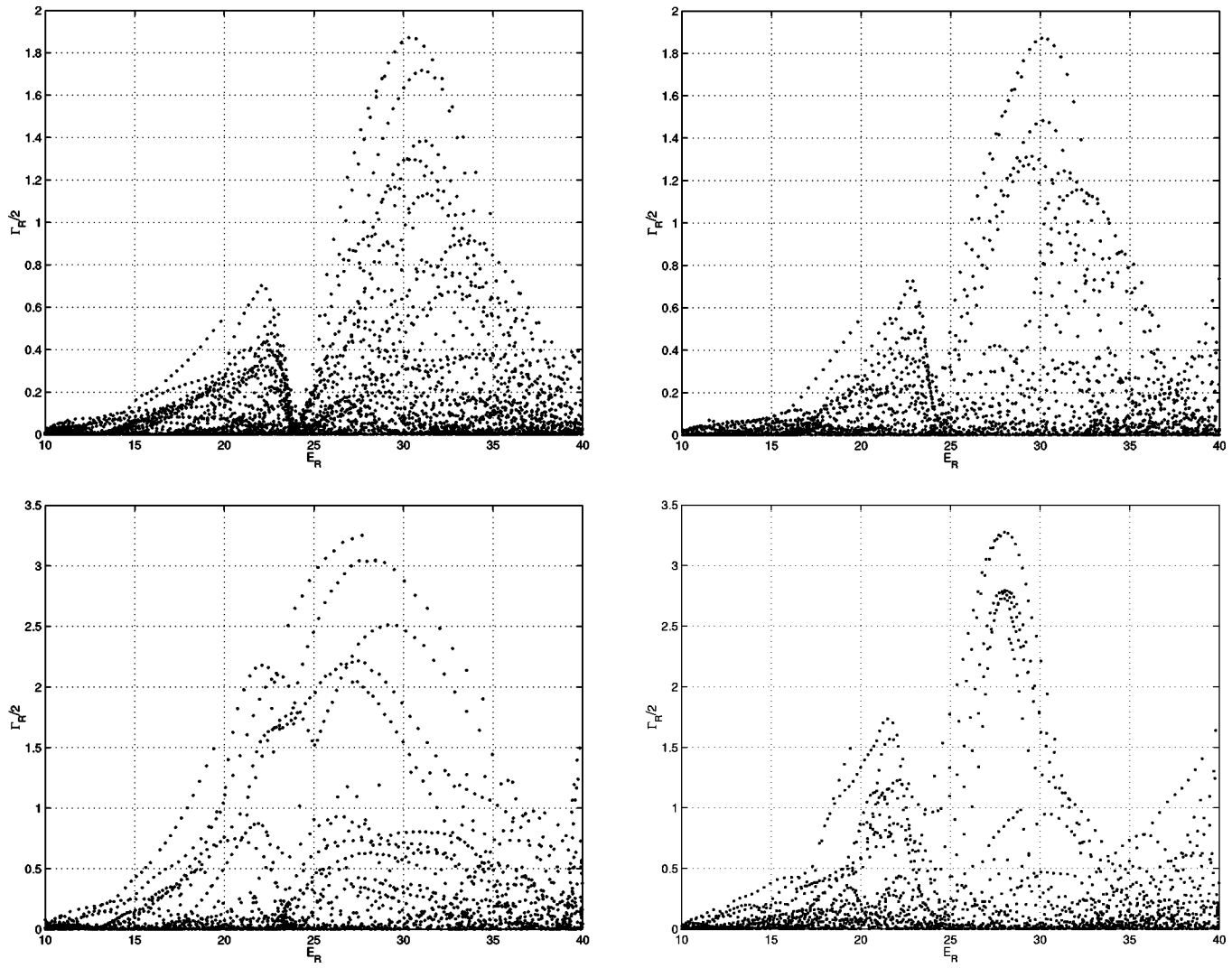

FIG. 3. Eigenvalue picture: motion of the poles of the S matrix in dependence on increasing length (left) ($y_d=-6.0{:}0.02{:}-3.0$ and $x_r=1.5$) and width (right) ($x_r=1.5{:}0.02{:}3.5$ and $y_d=-3.0$) of the resonator. The opening of the aperture is $w=0.15$ (top) and $w=0$ (bottom). The energies are given in units of $[x]^{-2}$.

B. Realistic cases

In Ref. [7], the behavior of poles of the S matrix in an open two-dimensional regular microwave billiard connected to a single waveguide is studied. As a function of the coupling strength between the resonator and the waveguide, the position of the corresponding resonance poles, the wave functions of the resonance states and the Wigner-Smith time delay function are calculated. The poles are calculated on the basis of the exterior complex scaling method. The energy of the incoming wave is chosen so that only the channel corresponding to the first transversal mode in the lead is open.

In Ref. [7], the bifurcation of the widths (resonance trapping) can be seen very clearly indeed. In particular, the contraintuitive result that the lifetimes of certain resonance states increase with increasing coupling to the continuum can be traced not only in the motion of the poles of the S matrix in the complex plane. It can also be seen in the wave functions of the resonance states and, above all, in the measurable time-delay function. In the case of three interfering resonance states, the wave function of (at most) one of the long-lived trapped states may be pure in relation to the bound states of the closed resonator [7]. More exactly, $b_{ii}=1$ at small and large coupling strength. Some mixing of all three wave functions appears in the critical region where the wave functions are biorthogonal ($B>1$).

Another example is the motion of the poles of the S matrix by varying the coupling strength between the states of an atom by means of a laser. In Ref. [3], the positions and widths of two resonances in the vicinity of an autoionizing state coupled to another autoionizing one (or a discrete state) by a strong laser field are considered. For different atomic parameters, the trajectories in the complex energy plane are traced by fixing the field frequency ω but varying the intensity I of the laser field. The states are coupled directly as well as via a common continuum and the ratio of these couplings is defined by the Fano parameter Q [16]. Most interesting is the region of avoided resonance crossing where the motion of each eigenvalue trajectory is influenced strongly by the motion of the other one. This occurs at a certain critical intensity I_{cr}. When furthermore the frequency is equal to the critical value ω_{cr}, then laser induced degenerate states arising at the double pole of the S matrix are formed. The strong correlation between the two states for intensities around I_{cr} reflects itself in the strong changes of the shape parameters

of the resonances in the cross section. It can therefore be traced.

In the limit of vanishing direct coupling ($Q \to 0$), the widths bifurcate at $I = I_{cr}$ as in other open quantum systems. This means that the width of one of the resonance states increases with increasing $I > I_{cr}$, while the width of the other decreases relative to the first one. In the limit $I \to \infty$, the ratio between the widths of the long- and short-lived states approaches zero (resonance trapping). This corresponds to the situation shown in Fig. 1(d). In the other limiting case, the coupling via the continuum vanishes (the Q value is large). Here the levels repel in their energetic positions when $I \geqslant I_{cr}$. This corresponds to Fig. 1(a).

In any case, i.e., for *all* Q values, the two resonance states start to repel each other in the *complex* energy plane at $I = I_{cr}$. The repulsion of the eigenvalues in the complex plane is an expression of the strong mutual influence of one state on the other one in the critical region around I_{cr}. In the transition region (Q values of the order of magnitude 1), the trajectories show a complicated behavior. Here population trapping may appear, i.e., the width of one of the resonance states may vanish at a certain finite intensity $I_{pt} > I_{cr}$. It appears, generally, if the process is neither pure level repulsion on the real axis nor pure resonance trapping, but the amplitudes of both processes (i.e., the direct coupling of the two states and their coupling via the continuum) are of comparable importance, and interfere with one another.

Thus the results obtained in Ref. [3] for two interacting atomic levels confirm qualitatively the results of the schematical study represented in Sec. III A, although not only the nondiagonal matrix elements of $\mathcal{H}^{\text{eff}}$ but also the width Γ_1 itself depend on I. These results and those for the microwave cavity discussed above show very clearly that individual resonance states can mix not only due to the two-body forces between the substituents of the system, *but also* as a consequence of avoided resonance crossings. Other realistic cases are the resonance doublet $J^{\pi} = 2^{+}$; $T = 0$; and 1 in the nucleus ^{8}Be, and the $\rho - \omega$ and the meson doublet $T = 1$; 0 [14].

In Ref. [15], the electric-field-dependent intrinsic lifetimes of resonances in biased multiple quantum wells are studied. Long-lived resonances typically exhibit an anticrossing of their eigenenergies and a crossing of their lifetimes, while short-lived resonances feature a crossing of their eigenenergies and an anticrossing of their lifetimes. This is in full agreement with the conditions $R > 0$ and $R < 0$ for an anticrossing and a crossing of the energies, respectively, following from Eq. (10). The first case is characterized by a swapping of positions under varying electric fields at the anticrossing, while the levels remain essentially localized in the second case even at the crossing.

IV. SPECTROSCOPIC PROPERTIES OF AN OPEN MICROWAVE RESONATOR

A. Calculations for the open microwave resonator

The calculations are performed for a rectangular flat resonator coupled to a waveguide. Inside the cavity, a circular scatter is placed. We use the Dirichlet boundary condition $\Phi = 0$ on the borders of the billiard and the waveguide. The waveguide has a width equal to 1, and is attached to the resonator through a slide with an adjustable opening (which is also described by the Dirichlet boundary condition). For $w = 0.5$ the resonator and the waveguide are disconnected, while $w = 0$ represents the maximal coupling (opening).

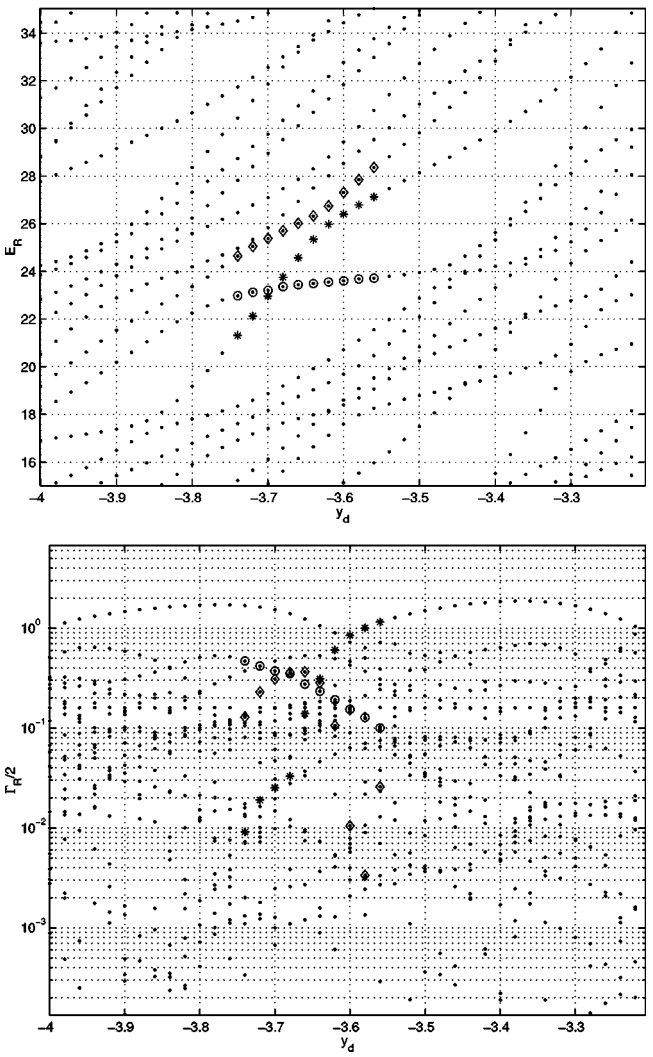

FIG. 4. Energies (top) and widths (bottom) as a function of y_d for $w = 0.15$ and $x_r = 1.5$. For ten values of y_d, the poles of three states are marked by diamonds (A), stars (B), and circles (C). It is $E_A > E_B > E_C$ and $\Gamma_B > \Gamma_C > \Gamma_A$ at $y_d = -3.56$, while $E_A > E_C > E_B$ and $\Gamma_C > \Gamma_A > \Gamma_B$ at $y_d = -3.74$. The wave functions of these three states are shown in Fig. 5.

The cavity has a minimum area 3×3 which is determined by $x_r = 1.5$ and $y_d = -3$ (compare Fig. 2). The area is varied by varying x_r or y_d, while both the position of the lead and the scatter inside the cavity remain unchanged.

We solve the equation $-\Delta\Phi = E\Phi$. Inside the waveguide, the wave function has the asymptotic form $\Phi = (e^{iky} - R(E)e^{-iky})u(x)$. Here $u(x)$ is the transversal mode in the waveguide, k is the wave number, and $R(E)$ is the reflection coefficient. The energies and widths of the resonance states are given by the poles of the coefficient $R(E)$ analytically continued into the lower complex plane. They are identical to the poles of the S matrix, when the fixed point equations for the $\tilde{E}_R$ and $\tilde{\Gamma}_R$ are solved (see Sec. II).

To find the poles we use the method of exterior complex scaling [17,18]. For details, see Ref. [8].

FIG. 5. The wave functions of the three states A (left), B (middle), and C (right) shown in Fig. 4 for $x_r=1.5$ and $y_d=-3.56$ (1), -3.58 (2), -3.60 (3), -3.62 (4), -3.64 (5), -3.66 (6), -3.68 (7), -3.70 (8), -3.72 (9), and -3.74 (10).

B. Resonances as a function of the area of the resonator

We studied the motion of the poles of the S matrix as a function of the area of the resonator by changing both its length y and width x. The changes of the corresponding wave functions Φ_R are traced. We studied the energy region between the two thresholds at $\pi^2 \approx 10$ and $(2\pi)^2 \approx 40$, where only one channel is open.

In Fig. 3, the eigenvalue picture is shown for $w=0.15$ (the aperture is partly closed by the slide) and $w=0$ (the aperture is fully open) for different values of the length and width of the resonator. In all cases, oscillations of the widths as a function of y_d or x_r in the energy region considered can be seen. The amplitudes of the oscillations are larger for larger widths. At $w=0.15$, all states corresponding to differ-

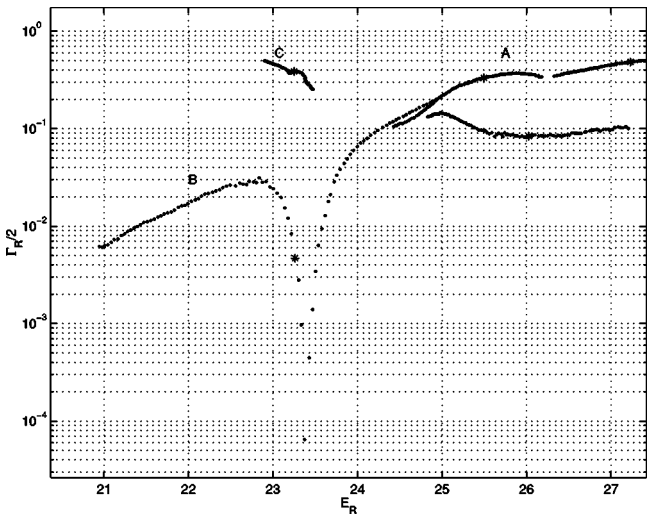

FIG. 6. Eigenvalue picture: motion of the poles of the S matrix in dependence on increasing length of the resonator ($y_d = -3.75:0.001:-3.65$). The eigenvalues at $y_d = -3.693$ are marked by stars. $w = 0.15$.

ent y_d ($-3 > y_d > -6$) and lying around 24 have small widths. This is caused, obviously, by certain symmetry properties of the wave functions in relation to the channel (since this energy is in the middle between the two thresholds). The minimum in the widths vanishes when the wave functions are strongly mixed via the continuum ($w = 0$). This shows that the coupling to the channel washes out some spectroscopic properties of the closed system.

For $w = 0.15$, the energies and widths of the states lying in the energy region around 24 are shown in Fig. 4 as a function of y_d. $E_R(y_d)$ show typical avoided crossings, while the picture of $\Gamma_R(y_d)$ is more complicated. For the three states denoted by diamonds, stars, and circles, respectively, the wave functions are shown in Fig. 5 for ten different neighboured values of y_d.

Two states (B and C) cross freely in the energy at $E_R \approx 23$. The wave functions of the two states B and C are very different from one another, and the interaction due to Re(W) between them is obviously small. The wave functions of both states almost do not change in the crossing region. Only in the widths can some repulsion be seen, obviously caused by Im(W). This can be seen from Fig. 6, where the results are shown from a calculation with smaller steps in y_d around the free crossing.

Around $E_R = 27$, state B avoids crossing in energy with the other state (A) at some value y_d^{cr} (around -3.63). In this region, the wave functions of both states become strongly mixed; their widths become comparable and cross. The repulsion in their energies can be seen. The avoided crossing is caused mainly by Re(W). Beyond the critical region, the wave functions of the two states remain mixed, although some hint of their exchange can be seen.

These results show that an avoided level crossing in the complex plane can be seen in the projection onto the energy axis or in the projection onto the width axis. In the first case, Re(W) dominates, while in the second case the mixing of the states occurs mainly due to Im(W).

According to the oscillations of the widths and the varying number of states as a function of the length or width of

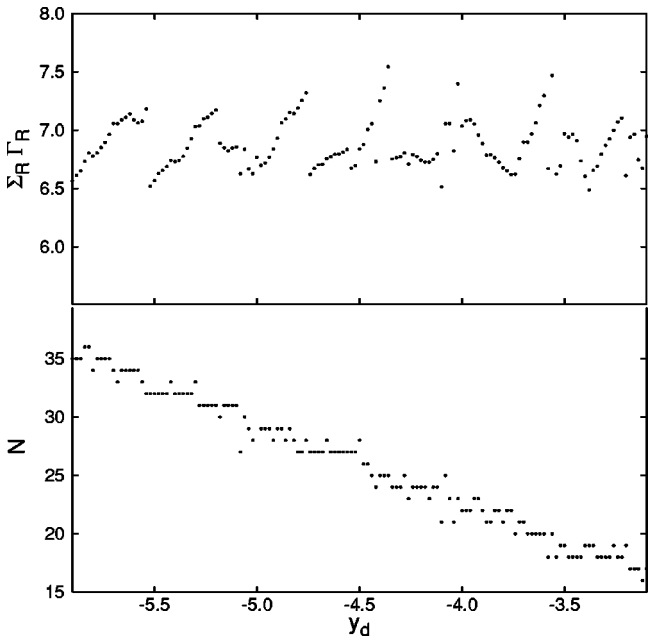

FIG. 7. The sum $\Sigma_R \Gamma_R$ of the widths (top) and the number N (bottom) of states lying between the two thresholds shown as a function of the length y_d of the cavity. $w = 0.15$.

the resonator, the sum of the widths of all states, lying between the two thresholds, fluctuates as a function of these values. In Fig. 7 (bottom), we show the number N of states as a function of y_d (for $w = 0.15$). This number increases since the number of states moving from above into the energy region considered is larger than the number of states leaving it to become bound. On the average, $\Sigma_R \Gamma_R$ is constant for a fixed value of w with fluctuations smaller than 10%. This can be seen from the example with $w = 0.15$ shown in Fig. 7 (top). The coupling of the cavity to the lead is therefore characterized by w but not by the area of the cavity.

C. Resonances as a function of the coupling strength to the lead

In Fig. 8, we show the eigenvalue picture obtained by varying w from 0.4 (almost closed aperture) to 0 (fully open aperture). The width of the resonator is determined by $x_r = 1.5$, and the length by the two neighboring values $y_d = -3.34$ (Fig. 8, top) and $y_d = -3.28$ (Fig. 8, bottom). In both cases, collective states are formed. They are formed in regions where the level density is comparably high. Even at a full opening of the aperture, collective states belonging to the different groups do not overlap. Thus they scarcely mix via the continuum.

In Fig. 9, we show the wave functions of the collective states from the lower part of Fig. 8. Although the wave functions of the collective states are very different from one another at a small opening of the aperture ($w = 0.4$), they are similar at a full opening ($w = 0$) [Figs. 9(d) and 9(f)], where they have large amplitudes near the aperture. The state shown in the middle [Fig. 9(e)] is trapped by the state to the left [Fig. 9(d)] at a comparably large opening (compare Fig. 8, bottom). The wave functions of the collective states at $w = 0$ in the long, and in the broad resonators ($x_r \to 4.0, y_d \to -6.0$) are also similar to those shown in Figs. 9(d) and 9(f).

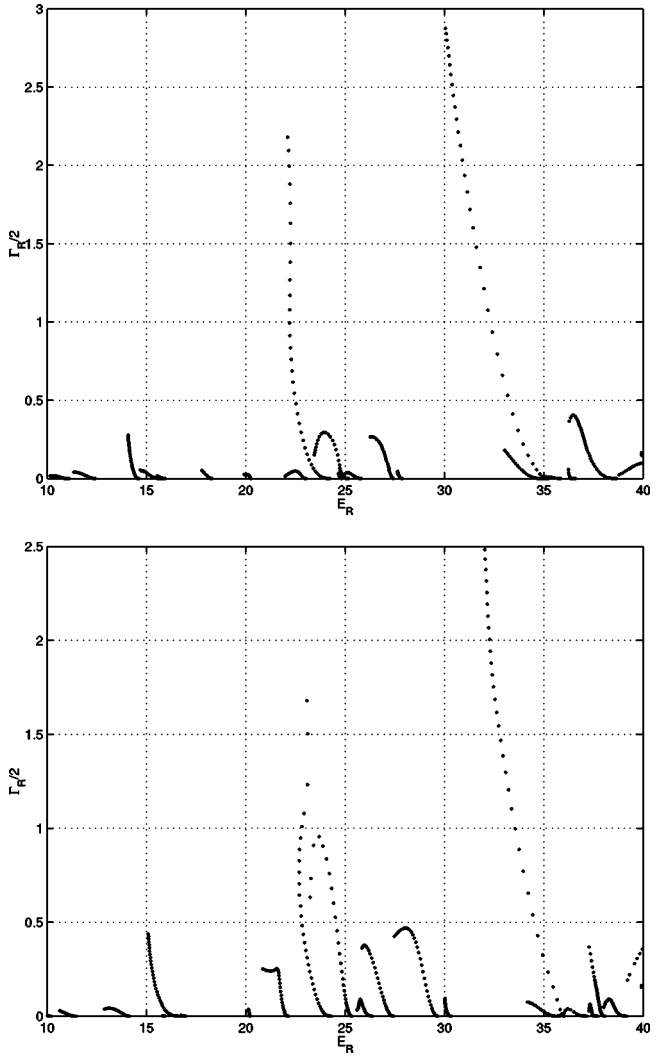

FIG. 8. Eigenvalue picture: motion of the poles of the S matrix in dependence on increasing opening (decreasing w; $w=0.4{:}0.01{:}0$) for $x_r=1.5$, $y_d=-3.34$ (top), and $y_d=-3.28$ (bottom).

D. Resonances and conductance of the resonator

The conductance of the resonator is described by the matrix elements $S_{cc'}$ [Eq. (5)], where c is the channel of the incoming wave and c' that of the outgoing wave. In our calculations, the second lead is on the lower right corner of the cavity, symmetrical to the first lead on the upper left corner. $x_r=1.5$ and $y_d=-3$.

In Fig. 10, the conductances at three different coupling strengths to the leads are shown together with the eigenvalue picture. In the eigenvalue picture, one can see the formation of two short-lived states at large openings (small w) in each group. This corresponds to the coupling of the resonator to two leads. It can be seen from the wave functions of the states that *both* short-lived states of each group are coupled strongly to *both* leads. The conductance is therefore large at large opening.

At low opening ($w=0.4$), the conductance peaks coincide with the resonance peaks. At larger opening ($w=0.2$ and 0), the conductance is an interference picture created by the overlapping resonances. The influence of the short-lived resonances onto the conductance can clearly be seen.

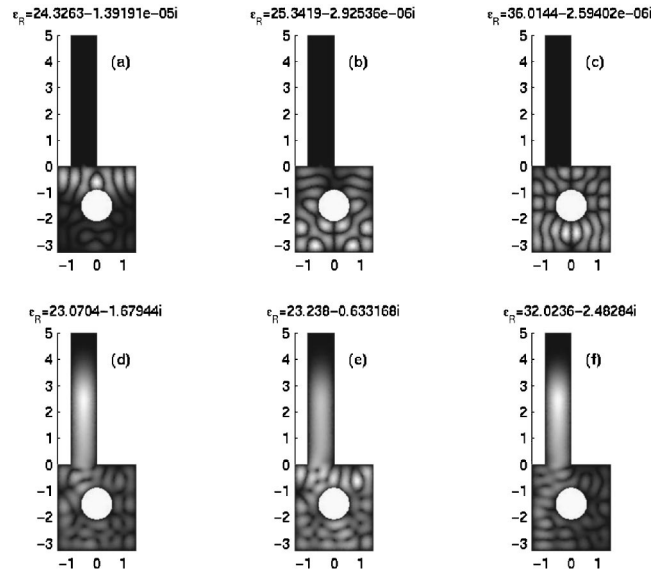

FIG. 9. The wave functions of the three broad states shown in the lower part of Fig. 8 at $w=0.4$ [(a)–(c)] and $w=0$ [(d)–(f)]. The state in the middle [(b) and (e)] becomes trapped by the state to the left [(a) and (d)].

In Fig. 11, the conductance is integrated over the energy of each group ($15\leqslant E\leqslant 25$ and $25\leqslant E\leqslant 40$), and plotted as a function of w. The conductance at the higher energy increases quite rapidly in a small region of w which corresponds to the critical region around w_{cr} (compare Ref. [8]).

V. DISCUSSION OF THE RESULTS

As demonstrated in Secs. III and IV, the wave functions of a quantum system mix under the influence of both the Hermitian and anti-Hermitian parts of the Hamiltonian. If the Hermitian part of the Hamiltonian is dominant, then an avoided crossing can be seen along the energy axis (*level repulsion*). If the anti-Hermitian part of the coupling via the continuum becomes important, then resonance trapping (*a bifurcation of the widths*) appears. In general, both types of mixing appear and may interfere. Note that this interaction between different states of a quantum system via the continuum does not require two-body forces between the constituents of the system.

The states whose wave functions are shown in Fig. 5 lie in an energy region around 24, where the coupling to the continuum is small. The mixing of the states is varied by means of varying the area of the resonator. In the upper part of the related Fig. 4, we see typical avoided level crossings in the energies $E_R(y_d)$. Here the widths of the two states become comparable to one another. This implies that $\mathrm{Re}(W)$ is decisive for the process. In this case, the results are similar to those known very well from studies on closed systems with discrete states (see Sec. III A).

However, we also see the opposite case: the crossing of the states B and C in Fig. 4 is free along the real axis, while the widths repel each other. In this case, $\mathrm{Re}(W)$ is obviously small [the wave functions of the two states are very different from one another (Fig. 5)]. Therefore, $\mathrm{Im}(W)$ is decisive, and the levels can, according to Sec. III A, cross along the real axis.

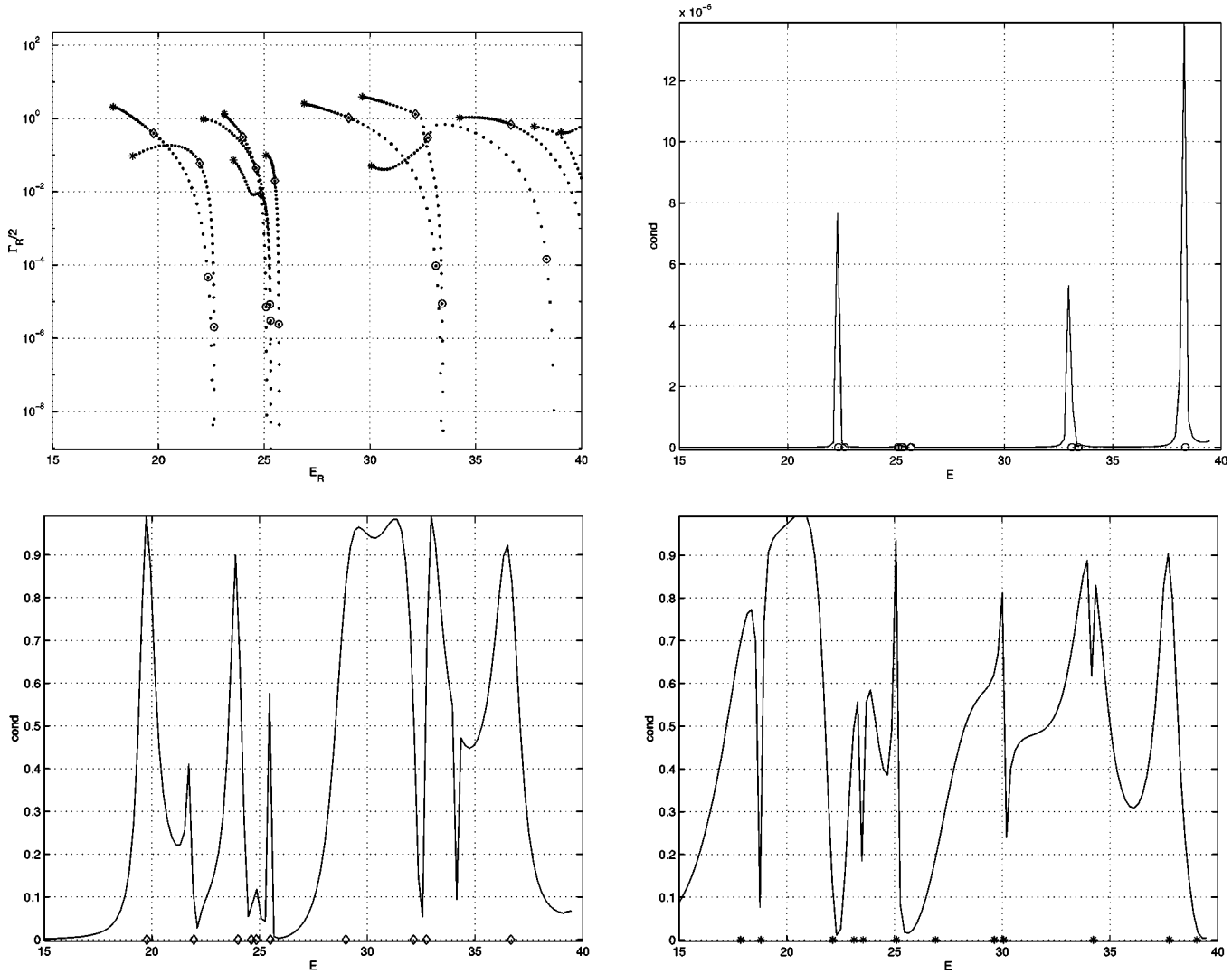

FIG. 10. Eigenvalue picture: motion of the poles of the S matrix in dependence on increasing opening (decreasing w, top left) and the conductance as a function of E for $w=0.4$ (top right), 0.2 (bottom left), and 0 (bottom right). The values $E_R-(i/2)\Gamma_R$ and E_R, respectively, for $w=0.4$, 0.2, and 0 are marked by circles, diamonds, and stars.

The variation of the widths of the resonance states as a function of the coupling strength to the continuum is traced in Fig. 8. In each group of overlapping states, one collective state is formed whose structure is determined by the channel wave function. This can be seen very clearly by comparing the wave functions of the different collective states, which are similar to one another but have almost nothing in common with the original wave functions of these states at small opening of the aperture (Fig. 9). Here the variation of the external mixing occurs mainly in the Im(W): the approaching of the states of a group in their positions as well as the trapping of all but one state inside each group due to enlarging Im(W) can be seen very clearly in Fig. 8.

It is interesting to compare Fig. 8 with the results for a slightly changed geometry of the cavity. In Ref. [8], the disk is smaller and all states between the two thresholds belong to one group. According to this, only one broad state is formed at full opening of the slide.

The avoided crossing of the two broad states in the lower part of Fig. 8 occurs according to the schematical picture with iw_{ex} [Fig. 1(d), level attraction and width bifurcation] with the only difference being that not only the nondiagonal

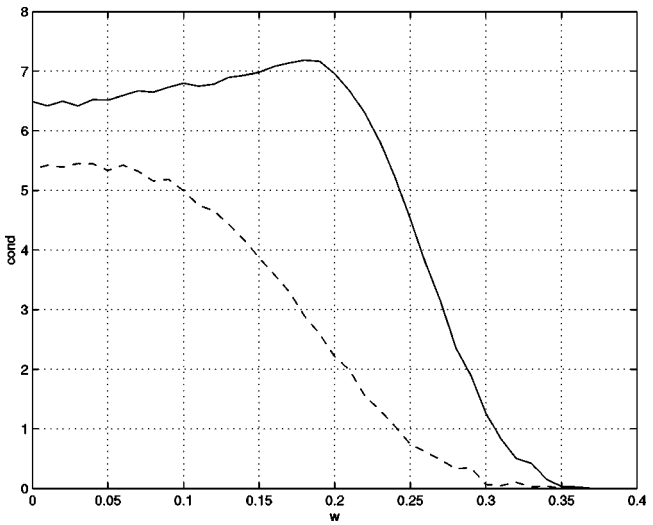

FIG. 11. Integrated conductance as a function of w in the energy region $25\leqslant E\leqslant 40$ (full line) and $15\leqslant E\leqslant 25$ (dashed line).

matrix elements of $\mathcal{H}$ depend on the coupling strength determined by w_{ex}, but also the diagonal ones. This case was studied in detail analytically and numerically in Ref. [11] in the framework of a schematical model.

In Ref. [9], avoided level crossings in a closed resonator under the influence of a driving field were studied. The results show avoided level crossings with and without a permanent mixing of the wave functions, in a similar manner as in the open resonator studied by us.

The relation between the peaks in the conductance, the Wigner delay times, and the positions of the states in the closed resonator was studied in Ref. [19]. The results of the present paper show that the conductance peaks are related to the positions of the resonance states in the *open* resonator. The peaks are, generally, the result of interferences between the resonance states.

Altogether, the interplay between Re(W) and Im(W) leads, as a rule, to permanent mixings of the wave functions. Level repulsion along the real axis is caused by Re(W), while a bifurcation of the widths (resonance trapping) is caused by Im(W). Both processes may interfere with one another. As a result, different time scales may appear and the energy dependency of the conductance changes with the degree of opening of the system in a non-trivial manner.

VI. CONCLUSIONS

The interaction W of resonance states via the continuum of decay channels consists of the Hermitian part Re(W) and the anti-Hermitian part Im(W). Both terms have to be considered not only in a many-body system [10] but also in the microwave billiard, as shown in the present paper. Some results show the dominance of Im(W), and others the dominance of Re(W). The avoided crossing of the resonance states in the complex plane may appear, under certain conditions, as a free crossing along the real axis or along the imaginary axis.

The interplay between the Hermitian and anti-Hermitian parts of the coupling operator between two resonance states via a common continuum may lead, in some cases, to a bifurcation of the widths (resonance trapping). In other cases, it may lead to a repulsion of the states along the real energy axis. The interaction W introduces, as a rule, permanent changes in the wave functions of the resonance states. Under certain conditions, the system may be stabilized dynamically [3].

The resonance picture of a microwave resonator shows all the characteristic features which are known from open quantum systems with two-body forces between the constituents. This result means that the interaction between the resonance states at the avoided level crossings in the complex plane plays an important role for a mixing of the wave functions. As an example, the wave functions of the collective short-lived states are strongly mixed in the set of wave functions of the closed system. They are quite different from those of the original states at small coupling to the continuum.

The statistical theory (random matrix theory) describes resonance states of an almost closed system. The poles of the S matrix are near to the real axis, and Im(W) is small. The effective Hamilton operator is $\mathcal{H}=\mathcal{H}_0+\mathrm{Re}(W)+\mathrm{Im}(W)=\mathrm{Re}(\mathcal{H})-iVV^{\dagger}$, where V's are the coupling vectors between discrete and scattering states [20]. The level repulsion along the real energy axis is embodied in Re($\mathcal{H}$) by choosing, e.g., the Gaussian orthogonal ensemble. Under these conditions, the effects caused by the interplay between Re($\mathcal{H}$) and Im($\mathcal{H}$) can be neglected to a good approximation. The results obtained in the present paper show, however, that the situation is different when the system is really open, i.e., when Im($\mathcal{H}$) and Re($\mathcal{H}$) are of the *same* order of magnitude. In this case, the interplay between the two parts of $\mathcal{H}$ causes *non-negligible* effects which are not considered in the statistical theory. The avoided crossing of resonance states in the complex plane embodies the interplay between resonance trapping and level repulsion along the real axis.

ACKNOWLEDGMENTS

Valuable discussions with J. Burgdörfer, M. Müller, J. Nöckel, K. Richter, and M. Sieber are gratefully acknowledged.

[1] V.V. Sokolov and V. Zelevinsky, Phys. Rev. C **56**, 311 (1997); E. Persson and I. Rotter, *ibid.* **59**, 164 (1999).

[2] V.V. Sokolov, I. Rotter, D.V. Savin, and M. Müller, Phys. Rev. C **56**, 1031 (1997); **56**, 1044 (1997).

[3] A.I. Magunov, I. Rotter, and S.I. Strakhova, J. Phys. B **32**, 1489 (1999); **32**, 1669 (1999).

[4] M. Desouter-Lecomte and J. Liévin, J. Chem. Phys. **107**, 1428 (1997); I. Rotter, *ibid.* **106**, 4810 (1997); M. Desouter-Lecomte and X. Chapuisat, Phys. Chem. Chem. Phys. **1**, 2635 (1999).

[5] Y.V. Fyodorov and H.J. Sommers, J. Math. Phys. **38**, 1918 (1997); T. Gorin, F.M. Dittes, M. Müller, I. Rotter, and T.H. Seligman, Phys. Rev. E **56**, 2481 (1997); E. Persson, T. Gorin, and I. Rotter, *ibid.* **58**, 1334 (1998); C. Jung, M. Müller, and I. Rotter, *ibid.* **60**, 114 (1999).

[6] W.D. Heiss, M. Müller, and I. Rotter, Phys. Rev. E **58**, 2894 (1998).

[7] E. Persson, K. Pichugin, I. Rotter, and P. Šeba, Phys. Rev. E **58**, 8001 (1998).

[8] P. Šeba, I. Rotter, M. Müller, E. Persson, and K. Pichugin, Phys. Rev. E **61**, 66 (2000).

[9] T. Timberlake and L.E. Reichl, Phys. Rev. A **59**, 2886 (1999).

[10] S. Drożdż, J. Okołowicz, M. Płoszajczak, and I. Rotter, Phys. Rev. C (to be published).

[11] M. Müller, F.M. Dittes, W. Iskra, and I. Rotter, Phys. Rev. E **52**, 5961 (1995).

[12] I. Rotter, Rep. Prog. Phys. **54**, 635 (1991).

[13] R.G. Newton, *Scattering Theory of Waves and Particles* (Springer, New York, 1982).

[14] P. von Brentano and M. Philipp, Phys. Lett. B **454**, 171 (1999),

and references therein.
[15] M. Wagner and H. Mizuta, Phys. Rev. B **48**, 14 393 (1993).
[16] U. Fano, Phys. Rev. **124**, 1866 (1961).
[17] B. Simon, Int. J. Quantum Chem. **14**, 529 (1978).
[18] A. Jensen, J. Math. Anal. Appl. **59**, 505 (1977).
[19] S. Ree and L.E. Reichl, Phys. Rev. B **59**, 8163 (1999).
[20] C. Mahaux and H. A. Weidenmüller, *Shell Model Approach to Nuclear Reactions* (North-Holland, Amsterdam, 1969).